GBP2 promotes clear cell renal cell carcinoma progression through immune infiltration and regulation of PD-L1 expression via STAT1 signaling

SHUJIANG YE[1,2*], SIYU LI[1,2*], LEI QIN[1,2], WEI ZHENG[1,2], BIN LIU[1,2], XIAOHUI LI[3], ZHENHUA REN[3], HUAIMING ZHAO[1,2], XUDONG HU[1,2], NAN YE[1,2] and GUANGYUAN LI[1,2,4,5]

[1]Department of Urology, The First Affiliated Hospital of Anhui Medical University; [2]Anhui Public Health Clinical Center, Hefei, Anhui 230012; [3]Department of Anatomy, School of Basic Medicine, Anhui Medical University, Hefei, Anhui 230032; [4]The Lu'an Hospital Affiliated to Anhui Medical University; [5]The Lu'an People's Hospital, Lu'an, Anhui 237005, P.R. China

Abstract. Guanylate-binding protein 2 (GBP2) has been widely studied in cancer, however, its potential role in clear cell renal cell carcinoma (ccRCC) is not fully elucidated. The present study aimed to explore the effect of GBP2 on tumor progression and its possible underlying molecular mechanisms in ccRCC. The Cancer Genome Atlas, Gene Expression Omnibus, Cancer Cell Line Encyclopedia databases, and several bioinformatics analysis tools, such as Gene Expression Profiling Interactive Analysis 2, Kaplan-Meier plotter, UALCAN, LinkedOmics, Metascape, GeneMANIA and Tumor Immune Estimation Resource, were used to characterize the functional relationship between GBP2 and ccRCC. Focusing on the association between GBP2 and programmed death ligand 1 (PD-L1) *in vitro*, the regulatory mechanism was investigated by knockdown and overexpression of GBP2 in Caki-1 and 786-O cells using reverse transcription-quantitative PCR, western blotting and co-immunoprecipitation techniques. The results indicated that GBP2 was commonly upregulated in ccRCC, correlating with worse prognosis. In addition, GBP2 expression levels were positively associated with different patterns of immune cell infiltration, suggesting that the GBP2 gene regulates PD-L1 expression via the signal transducer and activator of transcription 1 (STAT1) pathway. The present study suggested that GBP2 regulates tumor immune infiltration and promotes tumor immune escape through PD-L1 expression, revealing a potential immunotherapeutic target for ccRCC.

Correspondence to: Dr Guangyuan Li, Department of Urology, The First Affiliated Hospital of Anhui Medical University, 100 Huaihai Avenue, Hefei, Anhui 230012, P.R. China
E-mail: liguangyuanc@163.com

*Contributed equally

Introduction

Kidney cancer is one of the deadliest and most common diseases of the urology system, with ~179,368 deaths and 431,288 new cases worldwide as of 2020 (1). The most common type of kidney cancer is clear cell renal cell carcinoma (ccRCC), which accounts for ~70-75% of cases (2). ccRCC is characterized by aggressive tumors with a high metastatic rate and degree of immune infiltration, with tumor recurrence in 30% of patients who receive total nephrectomy (3,4). Immune therapies show great promise for patients with ccRCC. However, immunotherapy may not be appropriate for all patients, owing to low response rates (5). Therefore, identification of effective tumor immune-related therapeutic targets is of great clinical importance for treating metastatic ccRCC.

Guanylate-binding protein 2 (GBP2) is a member of the guanylate-binding protein (GBP) family (molecular weight of 65-67 kDa) and belongs to the dynamin superfamily of interferon-induced large GTPases (6,7). The GBP family is highly influential in mediating host defenses against cellular pathogens, parasites and viruses (8). Research has increasingly shown GBP2 to play an essential part in cancer. Several studies have revealed high rates of GBP2 expression in glioblastoma (9), pancreatic adenocarcinoma (10) and renal cell cancers (11), all of which share a poor prognostic outcome.

Immunosuppressive cell infiltration is a marker of altered therapeutic efficacy in ccRCC (12). Several studies have shown that degree of GBP2 expression is correlated with rate of tumor immune infiltration in breast cancer (13), colorectal cancer (14), pancreatic carcinoma (15) and sarcomas (16), indicating that GBP2 shapes the tumor immune microenvironment. High GBP2 expression may correlate with a favorable response to anti-PD-1 therapy and tumor-infiltrating T cell, with predicting favorable outcomes in breast cancer, colorectal cancer and sarcomas (13,14,16). On the contrary, GBP2 is correlated with acidosis-related high-risk group representing more tumor immune dysfunction and fewer immunotherapeutic responders in pancreatic carcinoma (15). These studies have illustrated that GBP2 can affect the prognosis of various tumors through regulating tumor immune microenvironment.

However, the function of GBP2 in immune infiltration, as well as its molecular regulatory mechanism in ccRCC, remain unclear.

GBP2, whose expression is significantly increased after interferon-γ (IFN-γ) treatment, is an interferon-stimulated gene (17). IFN-γ promotes tumor immune escape by upregulating programmed death ligand 1 (PD-L1) expression via the signal transducer and activator of transcription 1 (STAT1) pathway (18). According to several studies, PD-L1 expression positively correlates with metastasis and poor outcomes in ccRCC (19,20). A recent study indicated that GBP5 regulates PD-L1 expression levels in triple-negative breast cancer (21). Taken together, it was hypothesized that GBP2 may regulate PD-L1 expression via the STAT1 pathway, thereby promoting immune evasion in ccRCC.

In the present study, the potential role of GBP2 in immune infiltration of ccRCC along with its possible molecular roles were explored. To the best of our knowledge, this is the first study to demonstrate that GBP2 regulates PD-L1 expression via the STAT1 pathway. This finding expands our understanding of GBP2 immune infiltration mechanisms in ccRCC and provides a potential immunotherapeutic target.

Materials and methods

Cancer cell line encyclopedia (CCLE) database. The CCLE dataset (https://portals.broadinstitute.org/ccle) is an online database that provides analysis and visualization of more than 1,000 cell lines (22). The CCLE dataset provides information related to DNA mutations and gene expression. Based on this database, GBP2 expression levels in cancer cell lines were assessed (access date: 05/16/2021).

Gene expression profiling interactive analysis 2 (GEPIA 2) analysis. The online database GEPIA2 (http://gepia2. cancer-pku.cn/) is a website for analyzing differential gene expression, based on RNA sequencing data of 9,736 tumors and 8,587 normal samples from The Cancer Genome Atlas (TCGA) and Genotype-Tissue Expression (GTEx) (23). In the present study, the GBP2 expression level data on tumor and normal renal tissues and the correlation between GBP2 and PD-L1 were analyzed by this tool (access dates: 05/21/2021 and 05/03/2022).

Gene expression omnibus (GEO) dataset selection. Two microarray datasets were gained from the GEO database (http://www.ncbi.nlm.nih.gov/geo). Specifically, GSE6344 contains data for GBP2 mRNA between 20 ccRCC samples and 20 normal samples (24). GSE53757 contains data of GBP2 mRNA in 72 ccRCC and 72 normal samples (25). These two datasets were used to analyze the GBP2 mRNA levels in ccRCC and the dataset (GSE53757) to evaluate the correlation of GBP2 with PD-L1 (access date: 05/02/2022).

Kaplan-Meier (KM) plotter. KM plotter (https://kmplot. com/analysis) is able to evaluate the correlation between the expression of all genes and survival in 21 tumor types (26). The correlation between overall survival (OS) and GBP2 in ccRCC was performed using this online tool (access time: 05/16/2021).

UALCAN database. UALCAN (http://ualcan.path.uab. edu/index.html) is an online web with data obtained from 31 tumor types of TCGA project (27). The GBP2 expression in kidney renal clear cell carcinoma (KIRC) patients with different individual tumor stages, tumor grades, patient age, patient's sex and KIRC subtypes was analyzed using UALCAN (access date: 05/19/2021).

LinkedOmics database analysis. The LinkedOmics database (http://www.linkedomics.org/) is a public portal, which has the clinical data and multi-omics for 32 cancer types from TCGA (28). In the present study, the relation between GBP2 and KIRC was mainly evaluated. First, all genes co-expressed with GBP2 were obtained and showed as volcano plots. The top 50 genes that were positively and negatively associated with GBP2 were displayed in heat-maps (access date: 05/17/2021).

Metascape. Metascape (http://metascape.org) is a public online portal integrating a variety of bioinformatics knowledge databases for annotation and analysis of functional enrichment, gene annotation and protein-protein interaction (29). In the current study, based on GBP2-positively correlated genes (386 genes), Metascape was utilized to analyze the Gene Ontology (GO) and Kyoto Encyclopedia of Genes and Genomes (KEGG) of GBP2 gene (access date: 03/12/2022).

GeneMANIA database analysis. GeneMANIA (http://www. genemania.org) is a public online tool server used for analysis of genetic and protein interactions, co-expression, pathways and co-localization of target genes (30). The relationship between GBP2 and its interacting genes was analyzed using the aformentioned database (access date: 06/21/2021).

Tumor immune estimation resource (TIMER) database analysis. TIMER (https://cistrome.shinyapps.io/timer/) uses six state-of-the-art algorithms to assess immune infiltration levels (31). In the present study, the different expression GBP2 in tumors and adjacent tissues was first examined. Then, the correlations between the expression levels of GBP2 and infiltrating immune cells in KIRC were assessed. TIMER2.0 (http://timer.comp-genomics.org/) was also used to analyze the association between the expression of GBP2 and diverse immune cells gene markers in KIRC (access date: 06/20/2021) (32).

Clinical samples. The present study was approved [approval no. PJ-YX2022-016(F1)] by the Ethics Committee of the First Affiliated Hospital of Anhui Medical University (Hefei, China), which was conducted in accordance with the guidelines of the Declaration of Helsinki of 1975, as revised in 2000. The clinical sample included 40 specimens of ccRCC tissues, along with matched normal adjacent specimens, that were obtained from patients who received care at our hospital between January 2021 and August 2022. The patient donors (sex distribution, 67.5% men and 32.5% women; age range, 53-78 years) at the time of biopsy had not been treated with radiotherapy or chemotherapy. Written informed consent was provided by all patients. All of the tissue samples (paraffin-embedded) were used for immunohistochemistry (IHC); of these, six (gained with liquid nitrogen) were used in western blotting.

Cell cultures. Human 786-O and ACHN cell lines were purchased from Procell Life Sciences & Technology Co., Ltd. and were maintained in RPMI-1640 (Gibco; Thermo Fisher Scientific, Inc.) complete medium. A human proximal tubular epithelial cell line (HK2), along with human Caki-2, and Caki-1 cell lines were purchased from iCell Bioscience, Inc. The former was maintained in DMEM (Gibco; Thermo Fisher Scientific, Inc.), while the latter were maintained in McCoy's 5A (Procell Life Sciences & Technology Co., Ltd.) complete medium. Caki-1 (https://www.cellosaurus.org/CVCL_0234) and 786-O (https://www.cellosaurus.org/CVCL_1051) were described as RCC. ACHN (https://www.cellosaurus.org/CVCL_1067) and Caki-2 (https://www.cellosaurus.org/CVCL_0235) were described as papillary RCC (33,34). All complete medium was prepared with 10% fetal bovine serum (Gibco; Thermo Fisher Scientific, Inc.) and 1% antibiotics (100 μg/ml streptomycin and 100 U/ml penicillin). All cell lines were free of mycoplasma contamination and were cultivated in a 5% CO_2 incubator at 37°C. All cancer cell lines were identified with STR identification.

For inhibitor treatment, after GBP2 overexpressing, relevant cells were treated with 50 μM fludarabine (cat. no. T1038; TargetMol), a STAT1 inhibitor, for 36 h.

Construction and transfection of lentivirus. Lentivirus containing GBP2 shRNA and non-silencing (NS) control shRNA (shNS), as well as GBP2 overexpression (GBP2 OE) and negative control (vector) lentivirus, were produced by Shanghai GeneChem Co., Ltd. The shRNA target sequences were as follows: non-silencing (NS) control shRNA (shNS), 5'-TTCTCCGAACGTCACGT-3'; GBP2-RNAi (shGBP2#1), 5'-CTTTAGAAGAAGATGTCAA-3'; and GBP2-RNAi (shGBP2#2), 5'-TTTCGCTAAAGCTAAGAAA-3'. Transfection of the Caki-1 and 786-O cells was performed in accordance with manufacturer's instructions. Puromycin (2.0 μg/ml) was used to screen the infected cells for one week, and then analysis of silencing efficiency of target genes was performed by reverse transcription-quantitative PCR (RT-q) PCR and western blotting.

RNA interference. To knock down STAT1, Caki-1 and 786-O cells with GBP2 overexpression were transfected with small interfering (siRNA) using GP-Transfect-Mate (a transfection reagent; Shanghai GenePharma Co., Ltd.) according to the manufacturer's instructions. The sequences of siRNA (20 μM) used to target STAT1 and negative control, as customizing by Shanghai GenePhama Co., Ltd. were as follows: negative control (siNC), sense: 5'-UUCUCCGAACGUGUCACGUTT-3', antisense: 5'-ACGUGACACGUUCGGAGAATT-3'; siSTAT1#1, sense: 5'-GCUGGAUGAUCAAUAUAGUUT-3', antisense: 5'-ACUAUAUUGAUCAUCCAGCTT-3'; siSTAT1#2, sense 5'-G: ACCAUGCCUUUGGAAAGUTT-3', antisense: 5'-ACUUUCCAAAGGACUGGUCTT-3'. Analysis of silencing efficiency of target genes was performed by western blotting.

RT-qPCR. The RNA from cells was extracted using TRIzol® (cat. no. R0016; Beyotime Institute of Biotechnology). RNA purity (OD260 nm/OD280 nm=1.8-2.2) was evaluated using NanoDrop 2000 (Thermo Fisher Scientific, Inc.) and reversely

transcribed to cDNA with a reverse transcription kit (cat. no. 11139ES10; Yeasen Biotechnology Co., Ltd.) according to the manufacturer's instructions. qPCR was performed using SYBR Green Master Mix (cat. no. 11203ES03; Yeasen Biotechnology Co., Ltd.) in a fluorescence quantitative PCR instrument (CFX; Bio-Rad Laboratories, Inc.). The thermal cycling program was as follows: pre-denaturation for 30 sec at 95°C, denaturation for 15 sec at 95°C, and annealing and extension for 30 sec at 60°C, with repetition for 40 cycles. The primer sequences were as follows: GBP2 forward, 5'-CAGTTG GAAGCAAGGCGAGAT-3' and reverse, 5'-GCACCTCTT TGGCCTGTATCC-3'; PD-L1 forward, 5'-GCCGAAGTC ATCTGGACAAGC-3' and reverse, 5'-GTGTTGATTCTC AGTGTGCTGGTCA-3'; and β-actin forward, 5'-CACCCA GCACAATGAAGATCAAGAT-3' and reverse, 5'-CCAGTT TTTAAATCCTGAGTCAAGC-3'. Relative expressions levels were normalized to those of human β-actin. $2^{-\Delta\Delta Cq}$ method was used to analyze the data (35).

Western blotting. Protein lysates of tissues and cells were isolated using radioimmunoprecipitation assay buffer (cat. no. P0013B; Beyotime Institute of Biotechnology) containing protease and phosphatase inhibitors (cat. no. P1048; Beyotime Institute of Biotechnology), using the bicinchoninic acid (BCA) method (cat. no. P0012; Beyotime Institute of Biotechnology). The extracted protein lysate (10-50 μg) was transferred to nitrocellulose (NC) membranes (cat. no. 66485; Pall Life Sciences) after 8-10% SDS-PAGE electrophoresis. The NC membranes were blocked in 5% skimmed milk for 1 h at 20-25°C and were incubated for 8-12 h at 4°C with specific primary antibodies against STAT1 (1:1,000; cat. no. R25799), phosphorylated (p)-STAT1 (Ser727) (1:1,000; cat. no. R25797; both from Zen BioScience), PD-L1 (1:5,000; cat. no. 381830), β-actin (1:5,000; cat. no. 66009-1-lg), Flag (1:6,000; cat. no. 20543-1-AP) and GBP2 (1:1,000; cat. no. 27299-1-AP; all from Proteintech Group, Inc.). After incubation of the NC membranes with the secondary antibody (HRP-conjugated goat anti-rabbit IgG (1:5,000; cat. no. 511203); HRP-conjugated goat anti-mouse IgG (1:5,000; cat. no. 511103); both from Zen BioScience) for 2 h at 20-25°C, protein band signals were acquired using a Tanon 5200 system (Tanon Technology Co., Ltd.) and quantified with ImageJ software (version 1.40 g; National Institutes of Health).

IHC. Paraffin sections (3-5 μm) were immersed in xylene and ethanol in turn dewaxed and rehydrated and the antigen was repaired using 10 mM sodium citrate buffer (pH 6.0). H_2O_2 (3%) was added to the slices, which were incubated for 20 min at room temperature. After washing with phosphate buffered saline (PBS), the sections were incubated at 4°C for 8-12 h with the following primary antibodies: GBP2 (1:200; cat. no. 27299-1-AP), PD-1 (1:400; cat. no. 18106-1-AP) and CD8A (1:800; cat. no. 66868-1-lg; all from Proteintech Group, Inc.). After further PBS washing, the specimens were incubated with the secondary antibodies (1:1; MaxVision™ HRP-Polymer anti-Mouse/Rabbit IHC kit; cat. no. 5010; Fuzhou Maixin Biotech Co., Ltd.) at 37°C for 1 h. The sections were stained brown with 3,3'-Diaminobenzidine (DAB) solution (cat. no. PR30010; Proteintech Group, Inc.). After rinsing with tap water, the nuclei were stained with hematoxylin. After

rinsing with tap water, slices were dehydrated and sealed with gum. Results were observed under a microscope (VS200, Olympus Corporation) and positive staining rate was determined. The expression levels of GBP2, CD8A, and PD-1 in the pathological tissue samples were evaluated based on the intensity of staining and the percentage of positively stained cells. A total of five fields per slice were randomly examined under a light microscope at x400 magnification. IHC results were evaluated by two pathologists using a blind test. The scoring system involved multiplying the staining intensity by the number of cells with positive scores. Staining intensity: 0, no positive cells; 1, yellow staining; 2, light brown staining; and 3, dark brown staining. Percentage of cells with positive scores: 1, <25%; 2, 25-50%; 3, 51-75%; 4, >75%. Scores 0, 1, 2 and 3 indicated low expression levels, while scores 4, 6, 8, 9 and 12 indicated high expression levels.

Co-immunoprecipitation (CO-IP) assay. For each immuno-precipitation assay (IP), the proteins extracted from Caki-1 and 786-O cells cultured in 10-cm dishes were processed using a CO-IP kit (cat. no. P2181S; Beyotime Institute of Biotechnology) according to the manufacturer's protocol. Western blotting was used to detect the protein signals with appropriate antibodies.

Statistical analysis. GraphPad Prism 7.0 software (GraphPad Software, Inc. and SPSS 25.0 (IBM Corp.) were used for statistical analysis. Every experiment was repeated three times, and continuous variables were expressed as the mean ± standard deviation (SD). Differences between two groups were evaluated with two-tailed Student's t-tests (unpaired or paired) and one-way analyses of variance (ANOVA) were used to compare values across multiple groups, whose post hoc test is Tukey's multiple comparisons test. Spearman and Pearson correlation coefficient was utilized for correlation analysis. Pearson's χ^2 tests were performed on IHC data to analyze the correlation of GBP2 with PD-1 and CD8A. P<0.05 was considered to indicate a statistically significant difference. The significance of statistic was as follows: *P<0.05, **P<0.01 and ***P<0.001.

Results

Overexpression of GBP2 in ccRCC. First, TIMER data were used to assess the mRNA expression of GBP2 in different tumors and matched normal tissues. The results revealed that GBP2 expression was significantly higher in most tumors, including ccRCC (P<0.01) (Fig. 1A, shown in the red frame). CCLE analysis revealed that GBP2 was distinctively overexpressed in renal cancer cell lines, with GBP2 mRNA expression level ranking seventh among multiple cancer cell lines (Fig. 1B, shown in the red frame). To further identify the expression of GBP2 in the TCGA dataset and GTEx projects, GEPIA2 was used with results indicating that GBP2 expression in ccRCC (red box) was higher than that in normal tissue (grey box) (Fig. 1C). To further validate these data, GBP2 expression levels in the ccRCC samples were evaluated using the GEO datasets. The same change in trends as aforementioned were observed (Fig. 1D and E), specifically thatGBP2 mRNA levels in ccRCC tissue was overexpressed compared with adjacent

normal tissues. These data demonstrated that upregulation of GBP2 expression may be a vital part of ccRCC progression.

GBP2 expression is associated with the clinical characteristics of ccRCC patients. To explore the effects of GBP2 on ccRCC prognosis, an analysis of OS was performed using the KM plotter database. These data suggested that upregulation of GBP2 mRNA is associated with shorter OS in patients with ccRCC (P=0.0014) (Fig. 2A), implicating GBP2 in tumor growth in ccRCC. To further characterize the specificity of GBP2 in ccRCC, various clinicopathological features of KIRC samples from the TCGA database were analyzed using the UALCAN online tool. It was found that GBP2 is differentially expressed in tissue of different stages and tumor grade (Fig. 2B and C). GBP2 expression was also revealed to vary as a function of patient age and sex as well as KIRC subtypes of ccRCC (P<0.05) (Fig. 2D-F). Hence, GBP2 may serve as a potential diagnostic and prognostic biomarker in patients with ccRCC.

GBP2 co-expression genes and protein-protein interaction (PPI) networks in ccRCC. To explore the molecular regulatory mechanism of GBP2 in ccRCC, the LinkedOmics online tool was utilized to analyze the GBP2 co-expression pattern within the ccRCC cohort. As revealed in the volcano plot (Fig. 3A), GBP2 was positively and negatively associated with 6846 genes (dark red dots) and 4705 genes (dark green dots), respectively. The top 50 genes with positive and negative associations with GBP2 are demonstrated in the heat maps (Fig. 3B and C). The majority of 50 positively correlation genes belonged to the immunosuppressive related gene (LAG3, TIGIT, PDCD1) and IFN-γ related genes (IFNG, CXCR3, CXCL9, IRF1). This outcome is congruent with the data we obtained from GO and KEGG pathway analysis with Metascape when predicting the biological role and pathway enrichment of GBP2 and its related genes. More specifically, GO analysis identified that GBP2 and its associated genes are mainly involved in the regulation of T-cell activation and adaptive immune response. The KEGG pathway analysis revealed that GBP2 and its related genes were principal influence to natural killer cell-mediated cytotoxicity and the T-cell receptor signaling pathway (Fig. 3D). By expanding the T-cell receptor signaling pathway, it was found that GBP2 KEGG analysis was involved in PD-L1 expression and the PD-1 checkpoint pathway in cancer (Table SI), suggesting that GBP2 high expression is associated with immune infiltration in ccRCC.

Next, a PPI network for GBP2 was constructed using the GeneMANIA online tool to determine the scope of GBP2 involvement in carcinogenesis. The results revealed that GBP2 was strongly co-expressed with GBP1, STAT1, STAT2, IRF1 and other genes (Fig. 3E), suggesting that GBP2 may interact with these genes to promote tumor progression. These results demonstrated that GBP2 plays a potentially positive significant role in immune infiltration, leading to a poor prognosis for ccRCC.

Correlation between GBP2 and immune infiltration in ccRCC. To verify whether GBP2 influences immune infiltration in ccRCC, the association between GBP2 and different levels of immune cell functioning was investigated using the
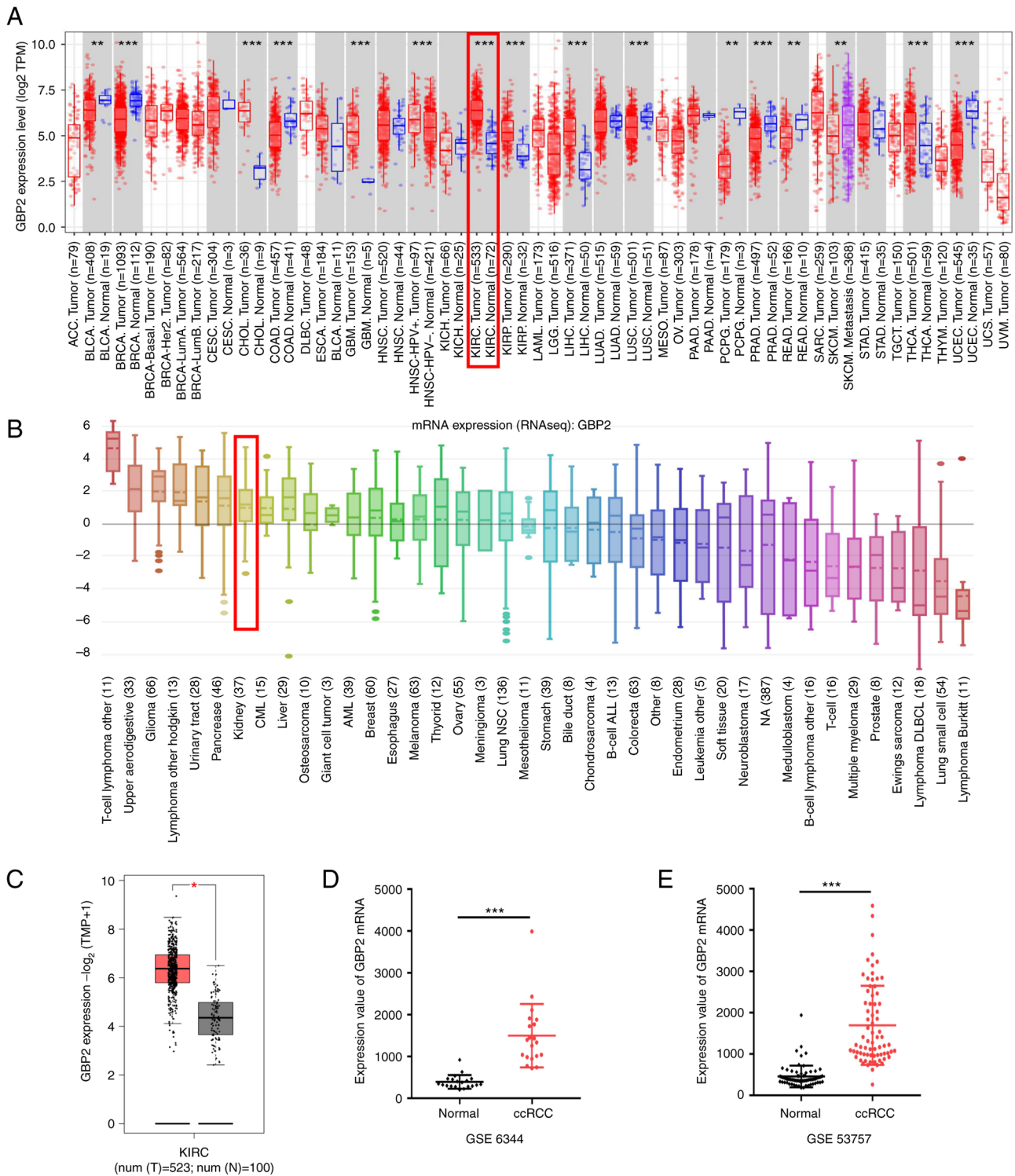
Figure 1. GBP2 expression in various tumors and cancer cell lines. (A) Expression of GBP2 mRNA in tumor and normal tissues was analyzed in Tumor Immune Estimation Resource 2.0. (B) The GBP2 mRNA expression levels of different cancer cell lines in Cancer Cell Line Encyclopedia. (C) The expression levels of GBP2 in kidney renal clear cell carcinoma and matched adjacent tissues using Gene Expression Profiling Interactive Analysis 2 online tool. (D and E) The GBP2 mRNA expression in ccRCC and matched adjacent tissues from GEO database [GEO: GSE6344 (n=20, D) and GEO: GSE53757 (n=72, E)]. *P<0.05, **P<0.01 and ***P<0.001. GBP 2, guanylate-binding protein 2; ccRCC, clear cell renal cell carcinoma; GEO, Gene Expression Omnibus.

TIMER online tool. It was found that GBP2 is a positively correlated with concentrations of immune cells in ccRCC (B cell: P=1.69x10^{-32}; CD8$^+$ T cell: P=1.69x10^{-43}; CD4$^+$ T cell: P=2.13x10^{-8}; macrophage: P=4.33x10^{-11}; neutrophil: P=1.50x10^{-32}; and dendritic cell: P=2.42x10^{-53}) (Fig. 4A), suggesting that GBP2 may participate in the immune immersion mechanism in ccRCC. TIMER2.0 was next used to analyze association of GBP2 with the expression of multiple immune cell markers (Table I). The outcomes verified the positive association between GBP2 and ccRCC-relevant gene markers for CD8$^+$ T cells, T-cells (general) and T-cell exhaustion.
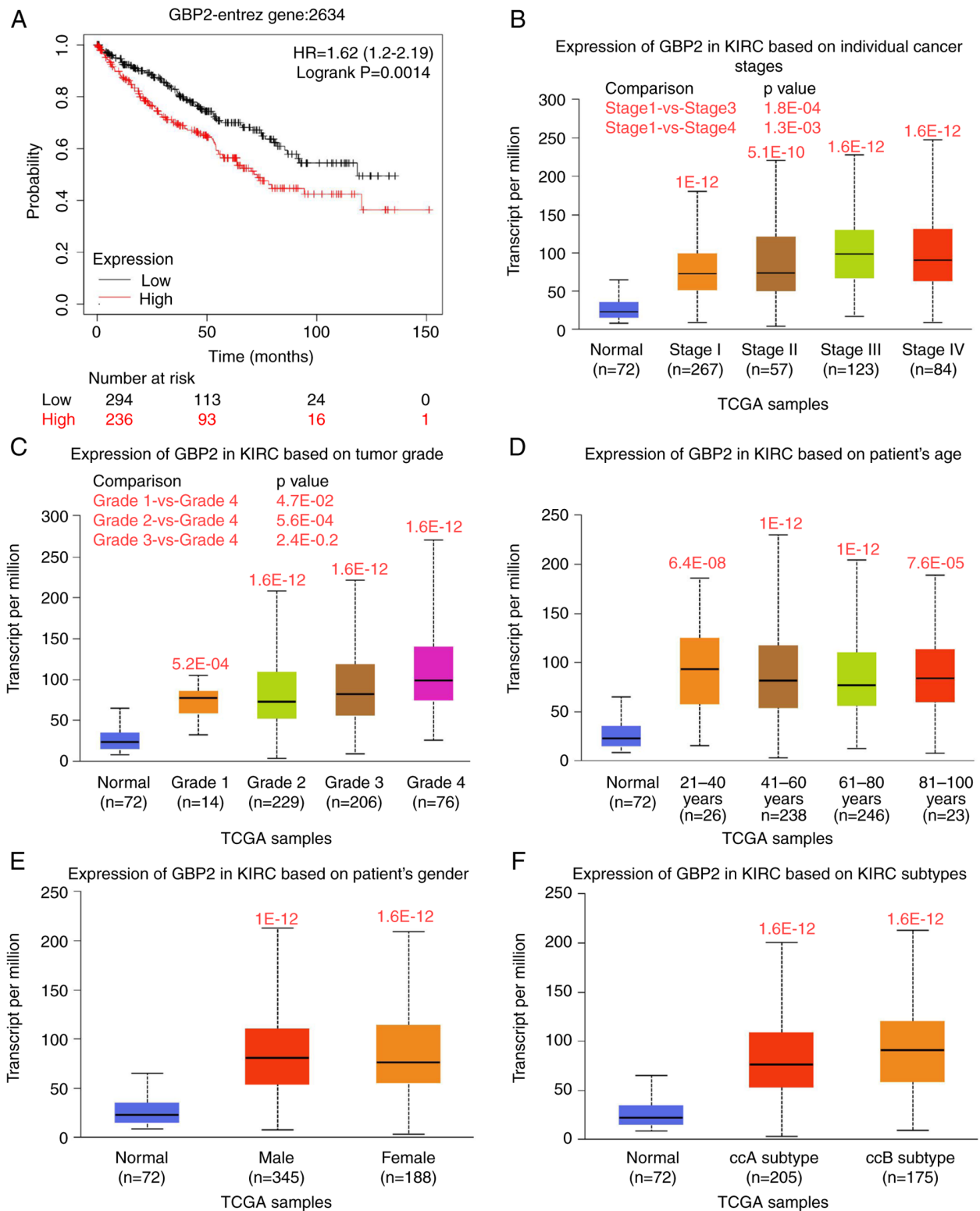
Figure 2. Clinical characteristics of GBP2 in ccRCC. (A) Survival curve of overall survival in ccRCC using Kaplan-Meier plotter database (n=530). (B-F) The association between GBP2 in KIRC expression with (B) individual cancer stages, (C) tumor grade, (D) patient's age, (E) patient's sex and (F) KIRC subtypes. GBP 2, guanylate-binding protein 2; ccRCC, clear cell renal cell carcinoma; KIRC, kidney renal clear cell carcinoma.

It was identified that GBP2 is highly correlated with CD8+ T-cell and T-cell exhaustion. Therefore, the relationship between GBP2 and CD8A (CD8+ T-cell marker gene) and PD-1 (T-cell exhaustion gene marker gene) was mainly explored using IHC. The results showed that GBP2, PD-1 and CD8A levels were greater in ccRCC samples than in the adjacent-normal reference samples (Fig. 4B). In addition, the expression levels of PD-1 (χ^2=4.821, P=0.028) and CD8A (χ^2=6.513, P=0.011) in the GBP2 high-expression group were significantly greater than those in the GBP2 low-expression group (Table II). Collectively, these data suggested that the oncogenic effect of GBP2 is relevant to antitumor immunity.
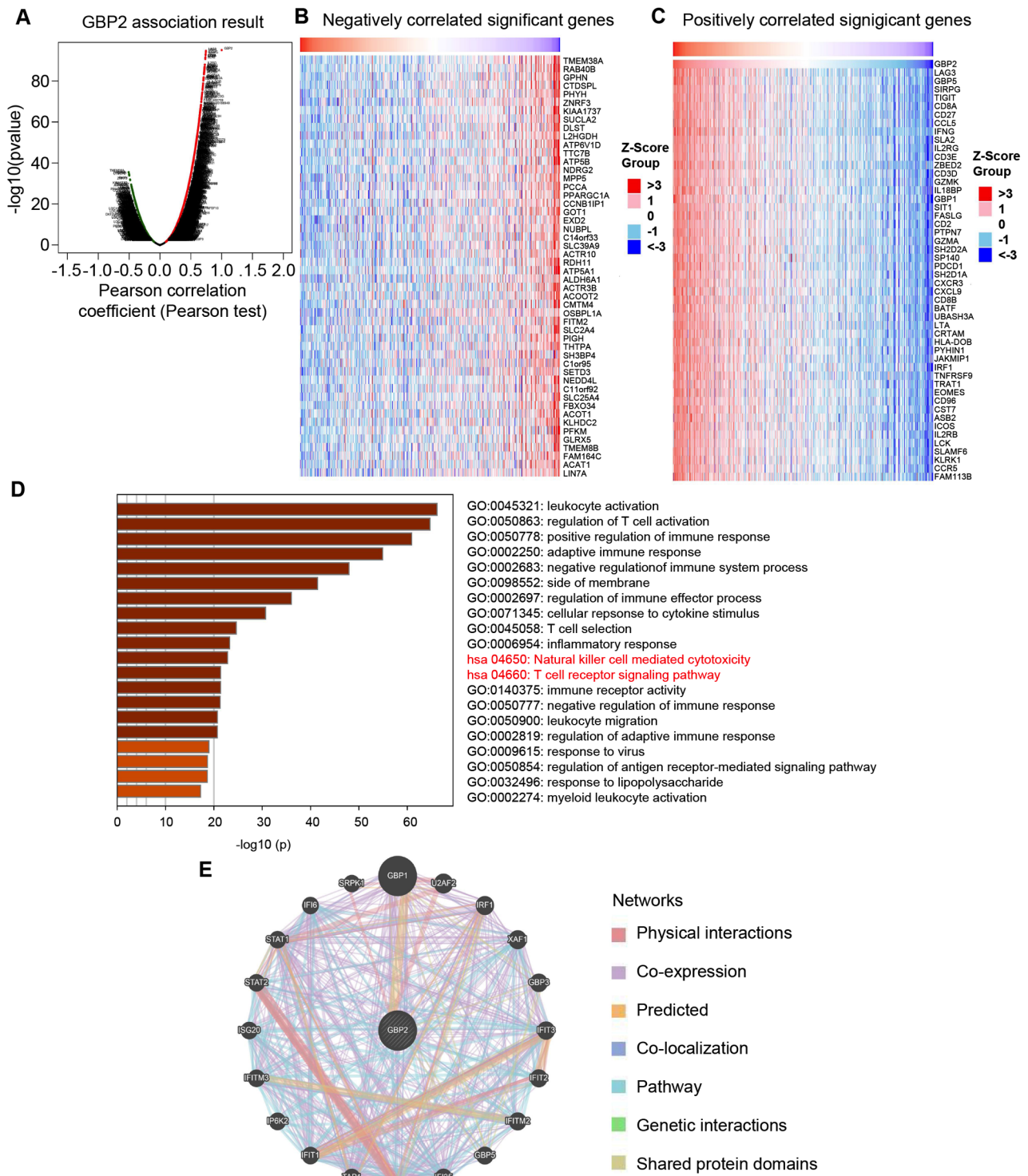
Figure 3. GBP2 co-expression genes and PPI network in KIRC. (A) The Pearson test in the KIRC cohort identified GBP2 highly associated genes. (B and C) Heat-maps showing the top 50 genes positively or negatively associated with GBP2 in KIRC. Positively and negatively associated genes were shown in red and blue, respectively. (D) Gene ontology and Kyoto Encyclopedia of Genes and Genomes analysis based on GBP2 positively correlated genes in Metascape. (E) PPI network of GBP2 in GeneMANIA. Each node represents a gene, and the size of the gene represents the strength of the interaction. GBP 2, guanylate-binding protein 2; PPI, protein-protein interaction; KIRC, kidney renal clear cell carcinoma.

Correlation between GBP2 and PD-L1 in ccRCC. Given that GBP2 was revealed to be highly correlated with T-cell exhaustion markers, the relationship between PD-L1 and GBP2 was further explored in the GEPIA2.0 database. Using the GEO dataset GSE53757, a significant positive correlation was detected between GBP2 and PD-L1 (GEPIA2: P=0.0088;

GSE53757: P<0.0001) (Fig. 4C and D). After adjusting for tumor purity, the same results were obtained in the TIMER database (P=1.30x10^{-3}) (Fig. 4E). To verify the aforementioned results, western blotting was performed on six pairs of ccRCC. GBP2 was found to be highly expressed in ccRCC tissue and positively correlated with concentration of PD-L1 (P=0.0102) (Fig. 4F).
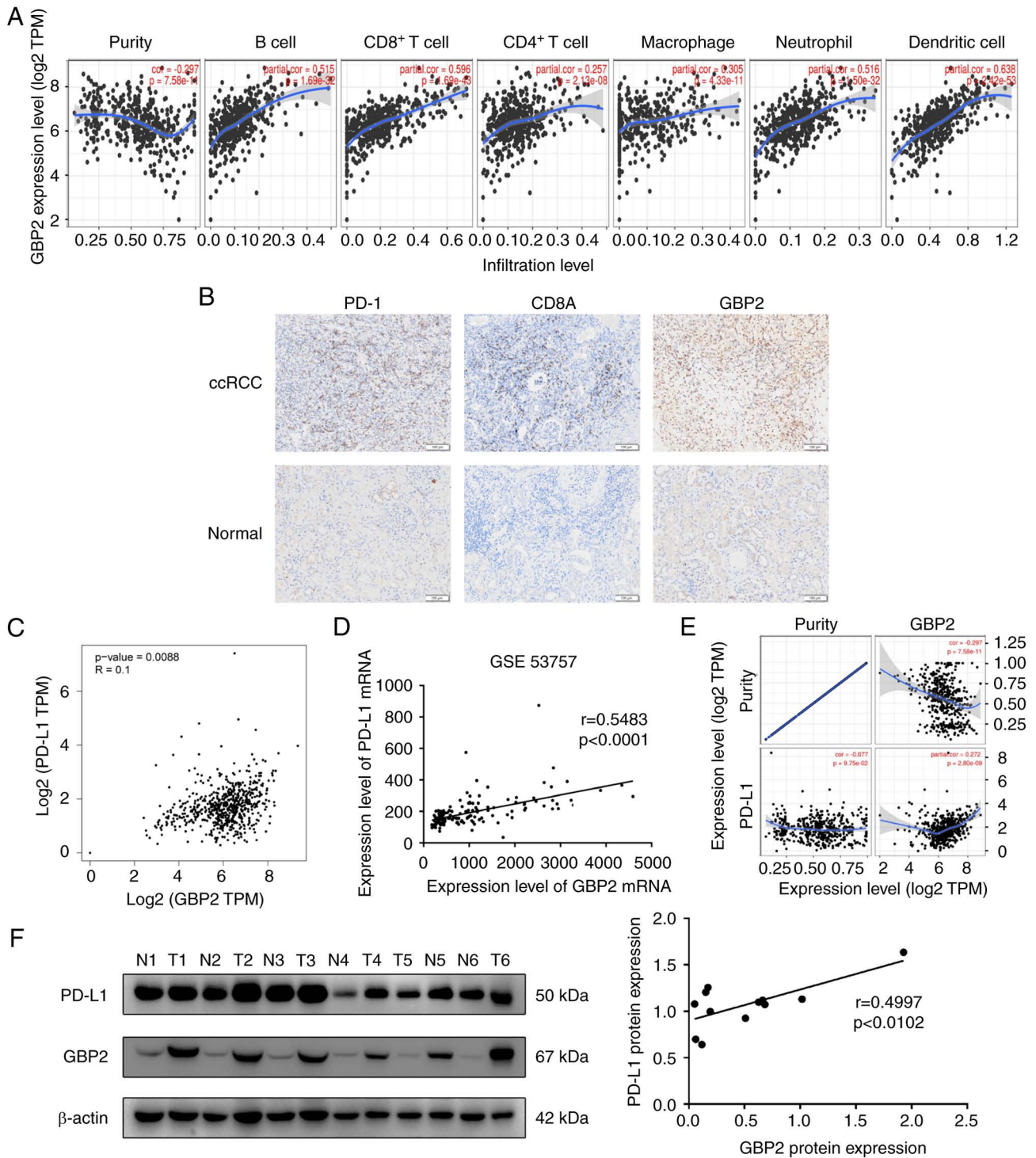
Figure 4. Correlations of GBP2 expression with immune infiltration in KIRC. (A) The TIMER database was used to analyze the correlation between GBP2 expression and immune infiltration in KIRC. (B) Immunohistochemistry revealed the expression levels of GBP2, CD8A and PD-1 in ccRCC tissues compared with adjacent normal tissues (n=40) (scale bar, 100 µm). (C-E) The association between GBP2 and PD-L1 was analyzed in the Gene Expression Profiling Interactive Analysis 2.0, Gene Expression Omnibus and TIMER databases. (F) Rates of PD-L1 and GBP2 expression in ccRCC and matched normal tissues were detected by western blotting. GBP 2, guanylate-binding protein 2; KIRC, kidney renal clear cell carcinoma; TIMER, Tumor Immune Estimation Resource; ccRCC, clear cell renal cell carcinoma; PD-L1, programmed death-ligand 1.

GBP2 regulation of PD-L1 expression. To investigate the effect of GBP2 protein on ccRCC, several *in vitro* experiments were conducted. First, GBP2 expression was examined in RCC cell lines using western blotting. The data indicated that, compared with normal renal tubular epithelial cells, GBP2 is overexpressed in renal cancer cells (P<0.05) (Fig. 5A). To assess the

effect of GBP2 on PD-L1 expression, GBP2 was knocked down or overexpressed in the Caki-1 and 786-O cell lines. To determine the efficiency of knockdown and overexpression, mRNA and GBP2 expression levels were verified with RT-qPCR and western blotting, respectively (Fig. S1A-H). Next, the mRNA expression of PD-L1 was examined using RT-qPCR in GBP2

Table I. Correlation analysis between guanylate-binding protein 2 and markers of immune cells in Tumor Immune Estimation Resource 2.0 database.

| Description | Gene markers | Kidney renal clear cell carcinoma | | | |
| | | None | | Purity | |
		Correlation coefficient	P-value	Correlation coefficient	P-value
CD8+ T cell	CD8A	0.720	<0.001	0.69	<0.001
	CD8B	0.677	<0.001	0.648	<0.001
T cell (general)	CD3D	0.686	<0.001	0.645	<0.001
	CD3E	0.702	<0.001	0.667	<0.001
	CD2	0.704	<0.001	0.662	<0.001
B cell	CD19	0.390	<0.001	0.33	<0.001
	CD79A	0.430	<0.001	0.382	<0.001
Monocyte	CD86	0.558	<0.001	0.517	<0.001
	CD115 (CSF1R)	0.441	<0.001	0.375	<0.001
TAM	CCL2	0.007	0.869	-0.062	0.183
	CD68	0.363	<0.001	0.343	<0.001
	IL10	0.489	<0.001	0.420	<0.001
M1 Macrophage	INOS (NOS2)	0.100	<0.01	0.063	0.175
	IRF5	0.224	<0.001	0.187	<0.001
	COX2 (PTGS2)	0.062	0.150	0.009	0.844
M2 Macrophage	CD163	0.389	<0.001	0.358	<0.001
	VSIG4	0.394	<0.001	0.335	<0.001
	MS4A4A	0.416	<0.001	0.368	<0.001
Neutrophils	CD66b (CEACAM8)	-0.020	0.651	-0.040	0.397
	CD11b (ITGAM)	0.394	<0.001	0.343	<0.001
	CCR7	0.472	<0.001	0.409	<0.001
Dendritic cell	HLA-DPB1	0.590	<0.001	0.574	<0.001
	HLA-DQB1	0.454	<0.001	0.400	<0.001
	HLA-DRA	0.589	<0.001	0.579	<0.001
	HLA-DPA1	0.618	<0.001	0.602	<0.001
	BDCA-1 (CD1C)	0.187	<0.001	0.112	<0.05
	BDCA-4 (NRP1)	0.147	<0.001	0.110	<0.05
	CD11c (ITGAX)	0.364	<0.001	0.328	<0.001
Th1	T-bet (TBX21)	0.396	<0.001	0.348	<0.001
	STAT4	0.472	<0.001	0.404	<0.001
	STAT1	0.662	<0.001	0.642	<0.001
	IFN-γ (IFNG)	0.723	<0.001	0.689	<0.001
	TNF-α (TNF)	0.320	<0.001	0.255	<0.001
Th2	GATA3	0.361	<0.001	0.356	<0.001
	STAT6	0.095	<0.05	0.111	<0.05
	STAT5A	0.518	<0.001	0.459	<0.001
	IL13	0.079	0.067	0.039	0.480
Tfh	BCL6	0.184	<0.001	0.175	<0.001
	IL21	0.224	<0.001	0.210	<0.001
Th17	STAT3	0.293	<0.001	0.271	<0.001
	IL17A	0.004	0.918	-0.034	0.464
Treg	FOXP3	0.547	<0.001	0.489	<0.001
	CCR8	0.554	<0.001	0.515	<0.001
	STAT5B	0.135	<0.01	0.146	<0.01
	TGFβ	0.237	<0.001	0.205	<0.001
T cell exhaustion	PDCD1	0.674	<0.001	0.644	<0.001
	CTLA4	0.568	<0.001	0.512	<0.001
	LAG3	0.700	<0.001	0.660	<0.001

Table I. Continued.

Description	Gene markers	Kidney renal clear cell carcinoma			
		None		Purity	
		Correlation coefficient	P-value	Correlation coefficient	P-value
	TIM-3 (HAVCR2)	0.295	<0.001	0.277	<0.001
	GZMB	0.411	0.366	0.366	<0.001

None, tumor purity was not used to adjust the results; purity, in the correlation analysis, the results were corrected by tumor purity.

Table II. The Pearson χ^2 test of GBP2, PD-1 and CD8A.

		GBP2 high (n=19)	GBP2 low (n=21)	χ^2	P-value
PD-1	High (n=18)	12	6	4.821	0.028
	Low (n=22)	7	15		
CD8A	High (n=21)	14	7	6.513	0.011
	Low (n=19)	5	14		

GBP2, guanylate-binding protein 2; PD-1, programmed death-1.

knockdown and overexpressing cells. It was demonstrated that mRNA expression of PD-L1 in ccRCC cells was significantly decreased in the Caki-1 and 786-O cells with GBP2 knockdown (P<0.01) (Fig. 5B). This change was reversed after overexpression of GBP2 (P<0.001) (Fig. 5C). Furthermore, western blotting results also showed that PD-L1 expression was regulated by GBP2 expression levels after GBP2 knockdown and overexpression in Caki-1 and 786-O cells (P<0.05) (Fig. 5D and E). These data suggested that GBP2 may regulate the expression of PD-L1 at the transcriptional level.

GBP2 regulates PD-L1 expression by interacting with STAT1. Next, the mechanism by which GBP2 regulates PD-L1 expression was investigated. Since it was found that GBP2 has a strong correlation with STAT1, and given that STAT1 has been revealed to promote the expression of PD-L1 (36,37), the effect of GBP2 on STAT1 was first investigated. Western blot analysis suggested that p-STAT1 (Ser 727) was downregulated after GBP2 knockdown in Caki-1 and 786-O cells (Fig. 6A). Furthermore, increased STAT1 phosphorylation was observed in Caki-1 and 786-O cells overexpressing GBP2 (Fig. 6B). To determine whether STAT1 is involved in GBP2 regulation of PD-L1, the GBP2-overexpressing cell lines were cultured with a STAT1 inhibitor (Fludarabine, 50 μM) and DMSO for 36 h. RT-qPCR data indicated that STAT1 inhibition weakened PD-L1 mRNA expression in Caki-1 and 786-O cells after GBP2 overexpression (P<0.01) (Fig. 6C). Furthermore, western blotting results suggested that PD-L1 levels were partially reduced when STAT1 was blocked (P<0.01) (Fig. 6D). To determine whether STAT1 plays a role in GBP2 regulation of PD-L1, STAT1 was silenced using siRNA in Caki-1 and 786-O cells. Western blotting was performed to determine the efficiency of STAT1 knockdown (Fig. S1I). Similarly,

by knocking down STAT1 in Caki-1 and 786-O cells overexpressing GBP2, it was found that upregulation of PD-L1 was reversed (P<0.05) (Fig. 6E). Importantly, the interaction between STAT1 and GBP2 was demonstrated by immunoprecipitation and western blot analysis in Caki-1 and 786-O cells overexpressing GBP2 (Fig. 6F). Based on these results, it was considered that GBP2 interacts with STAT1 and upregulates PD-L1 expression, which leads to tumor immune evasion and worsens the prognosis of patients with ccRCC (Fig. 6G).

Discussion

ccRCC, which is the main subtype of RCC, has a poor prognosis and lacks effective biological markers. Low rates of early diagnosis and scarcity of efficient therapies for patients with advanced or metastatic status are the leading causes of mortality in ccRCC (38,39). Therefore, validated early diagnosis, prognostic biomarkers and effective therapies are necessary to improve ccRCC outcomes. In the present study, GBP2 was identified as a new ccRCC biomarker and demonstrated that GBP2 acts in crucial ways in ccRCC. It was found that GBP2 is overexpressed in ccRCC tissue, suggesting poor prognosis, and that GBP2 overexpression, in turn, is correlated with immune infiltration. As revealed in the cell experiments, it was demonstrated that GBP2 regulates PD-L1 expression through the STAT1 pathway, thereby promoting tumor immune evasion and resulting in worse prognosis for ccRCC. In brief, the current results revealed that GBP2 may be a potential immunotherapeutic target in ccRCC.

Innate and adaptive immune cells interact with tumor cells through direct contact or through chemokine and cytokine signaling to shape the behavior of the tumor and its response to therapy (40). Tumor-infiltrating immune cells have been
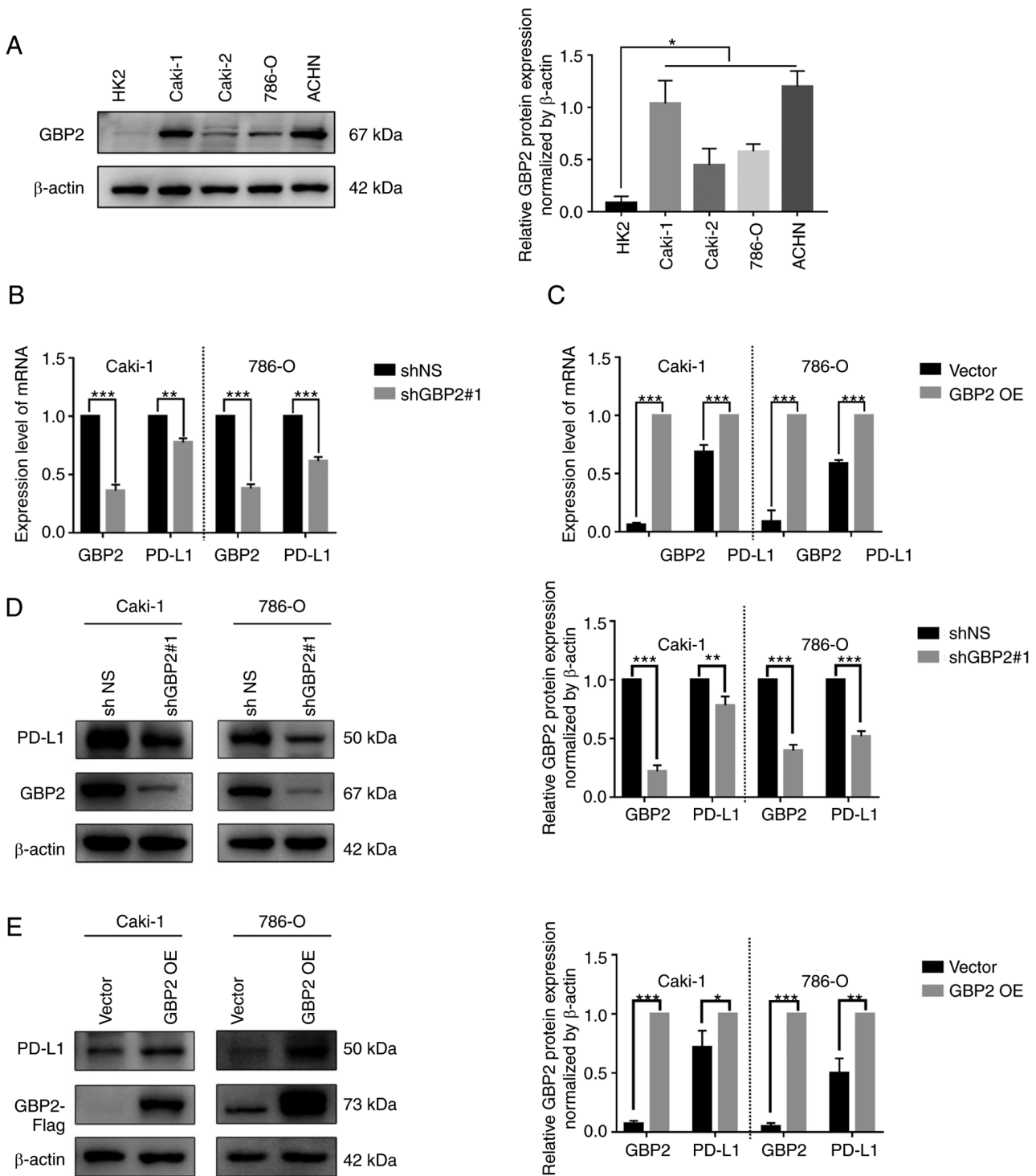
Figure 5. GBP2 regulates PD-L1 expression at mRNA and protein levels. (A) GBP2 expression in HK-2, Caki-1, Caki-2, 786-O, and ACHN was detected using western blotting. (B) PD-L1 and GBP2 mRNA expression were detected by RT-qPCR with shNS and shGBP2#1 in Caki-1 and 786-O cell lines. (C) PD-L1 and GBP2 mRNA expression were detected by RT-qPCR with vector and GBP2 OE in Caki-1 and 786-O. (D) PD-L1 and GBP2 protein expression were detected by western blotting with shNS and shGBP2#1 in Caki-1 and 786-O cell lines. (E) PD-L1 and GBP2 protein levels were detected by western blotting with vector and GBP2 OE in Caki-1 and 786-O cell lines. Data are expressed as the mean ± SD of three independent experiments. *P<0.05, **P<0.01 and ***P<0.001. GBP 2, guanylate-binding protein 2; PD-L1, programmed death-ligand 1; RT-qPCR, reverse transcription-quantitative PCR; OE, overexpression; sh-, short hairpin.

identified as potential biomarkers for cancer treatments (41). The present results revealed that GBP2 co-expressed genes are associated with features of the immune microenvironment of tumor cells as well as the immune response. In addition, GBP2 expression is moderately to highly correlated with a variety of immune cell markers, including CD8^{+} T cells, monocytes, M2

macrophages, Th2, Treg and T-cell exhaustion. This is consistent with the present IHC results, in which GBP2 was found to be correlated with PD-1 and CD8A expression in ccRCC. Previous studies have shown that patients with ccRCC who have a high degree of PD1^{+}, CD8^{+} T cells and Treg immune cells infiltration have a poor prognosis (42-44). Paradoxically,
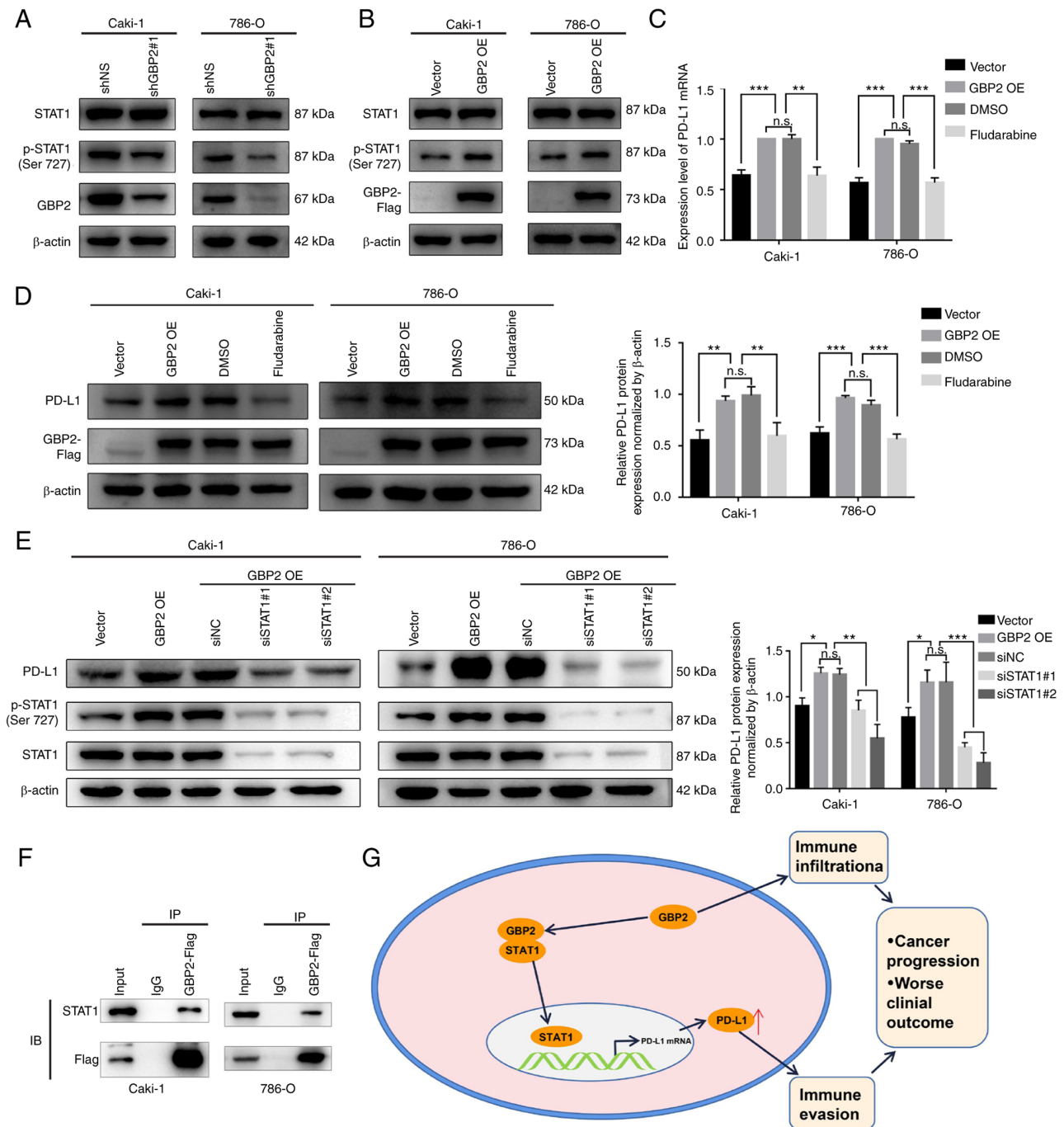
Figure 6. GBP2 regulates PD-L1 expression by interacting with STAT1. (A) Protein levels of GBP2, STAT1 and p-STAT1 (Ser 727) were examined by western blotting with shNS and shGBP2#1 in Caki-1 and 786-O cell lines. (B) Protein expression of GBP2, STAT1 and p-STAT1 (Ser 727) were examined by western blotting with vector and GBP2 OE in Caki-1 and 786-O cells. (C) Caki-1 and 786-O cells were treated with DMSO or Fludarabine (50 μM) for 36 h prior examining PD-L1 mRNA levels by reverse transcription-quantitative PCR. (D) Caki-1 and 786-O cells were treated with DMSO or Fludarabine (50 μM) for 36 h prior to immunoblot analysis of PD-L1 and GBP2 levels. (E) Concentrations of PD-L1, STAT1 and p-STAT1 were examined by western blotting in Caki-1 and 786-O (vector, GBP2 OE and GBP2 OE cells transfected with siNC or siSTAT1#1 and siSTAT1#2). (F) The protein-protein interaction between GBP2 and STAT1 was validated using immunoprecipitations followed by western blot analyses with indicated antibodies in Caki-1 cells and 786-O cells. IgG was used as an immunoprecipitation control. (G) A possible mechanism for GBP2-promoted PD-L1 upregulation and immunosuppression in clear cell renal cell carcinoma. Data are expressed as the mean ± SD of three independent experiments. *P<0.05, **P<0.01 and ***P<0.001. GBP 2, guanylate-binding protein 2; PD-L1, programmed death-ligand 1; p-, phosphorylated; sh-, short hairpin; OE, overexpression; si-, small interfering; NC, negative control; n.s., not significant.

in the tumor microenvironment of ccRCC, highly infiltrating CD8^{+} T cells could not improve prognosis, possibly due to exhaustion of CD8^{+} T cells (45).

In the present study, bioinformatics analysis revealed a high correlation between GBP2 and STAT1, and cell experiments indicated that GBP2 affects the phosphorylation of STAT1 *in vitro*. Activation of the STAT1 pathway in multiple tumor tissues indicates worse clinical outcomes, and STAT1 inhibition is sensitive to radiotherapy and chemotherapy in RCC (46,47). The aforementioned analysis indicated that GBP2 may activate STAT1 and lead to poor prognosis in ccRCC.

The immune checkpoint PD-L1 plays a vital role in promoting tumor immune escape (48). PD-L1 expression is regulated by multiple mechanisms; notably, STAT1 binds to the PD-L1 promoter and upregulates PD-L1 expression at the transcriptional level, thereby promoting tumor progression (36,49,50). In the present study, it was found that GBP2 regulates PD-L1 expression through the STAT1 pathways at the transcriptional and protein levels, and, moreover, that GBP2 interacts with STAT1, which was similar to certain previous studies (36,51). The aforementioned analysis suggested that GBP2 influences tumor escape by upregulating PD-L1 expression, thereby promoting tumor progression and worsening clinical prognosis in ccRCC.

However, the present study has certain limitations. Firstly, the public data information on ccRCC used in the current analysis was insufficient and could lead to potential errors/biases. Second, the tumor-promoting effect of GBP2 was only verified through *in vitro* experiments, without corollary *in vivo* data. Third, since PD-L1 is regulated by multiple mechanisms, additional research is needed to determine whether STAT1 binds to PD-L1 promoter and GBP2 governs PD-L1 expression beyond the STAT1 pathway in ccRCC.

Through a range of bioinformatics analyses and *in vitro* experiments, it was demonstrated that GBP2 is overexpressed in ccRCC. Furthermore, GBP2 overexpression is correlated with immune infiltration in renal cancer cells. It was further indicated that GBP2-mediated signaling via STAT1 induces PD-L1 expression, which may play an essential role in immune evasion in ccRCC. Hence, GBP2 may serve as an adverse prognostic marker and a potential immunotherapeutic target in ccRCC.

Acknowledgements

Not applicable.

Availability of data and materials

The datasets used and/or analyzed during the current study are available from the corresponding author on reasonable request.

Authors' contributions

SY, SL and GL conceived the idea and wrote the manuscript and confirm the authenticity of all the raw data. SY, LQ and HZ performed bioinformatics analysis. SY, WZ, BL and XH performed experimental validation. NY, XL, ZR and GL performed certain of the experiments in this study, revised the manuscript and supervised the study, as well as provided experimental technical support. All authors participated in the manuscript preparation, proofreading and submission. All authors read, confirmed, and approved the final version of the manuscript and agree to take responsibility for the contents of the article.

Ethics approval and consent to participate

The present study was approved [approval no. PJ-YX2022-016(F1)] by the Ethics Committee of the First Affiliated Hospital of Anhui Medical University (Hefei, China) and carried out in accordance with ethical standards of the Declaration of Helsinki. Written informed consent was obtained from each patient.

Patient consent for publication

Not applicable.

Competing interests

The authors declare that they have no competing interests.

References

1. Sung H, Ferlay J, Siegel RL, Laversanne M, Soerjomataram I, Jemal A and Bray F: Global cancer statistics 2020: GLOBOCAN estimates of incidence and mortality worldwide for 36 cancers in 185 countries. CA Cancer J Clin 71: 209-249, 2021.
2. Shuch B, Amin A, Armstrong AJ, Eble JN, Ficarra V, Lopez-Beltran A, Martignoni G, Rini BI and Kutikov A: Understanding pathologic variants of renal cell carcinoma: Distilling therapeutic opportunities from biologic complexity. Eur Urol 67: 85-97, 2015.
3. Braun DA, Hou Y, Bakouny Z, Ficial M, Sant' Angelo M, Forman J, Ross-Macdonald P, Berger AC, Jegede OA, Elagina L, et al: Interplay of somatic alterations and immune infiltration modulates response to PD-1 blockade in advanced clear cell renal cell carcinoma. Nat Med 26: 909-918, 2020.
4. Choueiri TK and Motzer RJ: Systemic therapy for metastatic renal-cell carcinoma. N Engl J Med 376: 354-366, 2017.
5. Choueiri TK, Fishman MN, Escudier B, McDermott DF, Drake CG, Kluger H, Stadler WM, Perez-Gracia JL, McNeel DG, Curti B, et al: Immunomodulatory activity of nivolumab in metastatic renal cell carcinoma. Clin Cancer Res 22: 5461-5471, 2016.
6. Praefcke GJK and McMahon HT: The dynamin superfamily: Universal membrane tubulation and fission molecules? Nat Rev Mol Cell Biol 5: 133-147, 2004.
7. Vestal DJ: The guanylate-binding proteins (GBPs): Proinflammatory cytokine-induced members of the dynamin superfamily with unique GTPase activity. J Interferon Cytokine Res 25: 435-443, 2005.
8. Tretina K, Park ES, Maminska A and MacMicking JD: Interferon-induced guanylate-binding proteins: Guardians of host defense in health and disease. J Exp Med 216: 482-500, 2019.
9. Yu S, Yu X, Sun L, Zheng Y, Chen L, Xu H, Jin J, Lan Q, Chen CC and Li M: GBP2 enhances glioblastoma invasion through Stat3/fibronectin pathway. Oncogene 39: 5042-5055, 2020.
10. Liu B, Huang R, Fu T, He P, Du C, Zhou W, Xu K and Ren T: GBP2 as a potential prognostic biomarker in pancreatic adenocarcinoma. Peerj 9: e11423, 2021.
11. Liu QY, Hoffman RM, Song J, Miao S, Zhang J, Ding D and Wang D: Guanylate-binding protein 2 expression is associated with poor survival and malignancy in clear-cell renal cell carcinoma. Anticancer Res 42: 2341-2354, 2022.
12. Diaz-Montero CM, Rini BI and Finke JH: The immunology of renal cell carcinoma. Nat Rev Nephrol 16: 721-735, 2020.
13. Junjun S, Yangyanqiu W, Jing Z, Jie P, Jian C, Yuefen P and Shuwen H: Prognostic model based on six PD-1 expression and immune infiltration-associated genes predicts survival in breast cancer. Breast Cancer 29: 666-676, 2022.
14. Wang H, Zhou Y, Zhang Y, Fang S, Zhang M, Li H, Xu F, Liu L, Liu J, Zhao Q and Wang F: Subtyping of microsatellite stability colorectal cancer reveals guanylate binding protein 2 (GBP2) as a potential immunotherapeutic target. J Immunother Cancer 10: e004302, 2022.

15. Tang P, Qu W, Wu D, Chen S, Liu M, Chen W, Ai Q, Tang H and Zhou H: Identifying and validating an acidosis-related signature associated with prognosis and tumor immune infiltration characteristics in pancreatic carcinoma. J Immunol Res 2021: 3821055, 2021.
16. Chen H, Song Y, Deng C, Xu Y, Xu H, Zhu X, Song G, Tang Q, Lu J and Wang J: Comprehensive analysis of immune infiltration and gene expression for predicting survival in patients with sarcomas. Aging (Albany NY) 13: 2168-2183, 2020.
17. Haque M, Siegel RJ, Fox DA and Ahmed S: Interferon-stimulated GTPases in autoimmune and inflammatory diseases: Promising role for the guanylate-binding protein (GBP) family. Rheumatology (Oxford) 60: 494-506, 2021.
18. Chen S, Crabill GA, Pritchard TS, McMiller TL, Wei P, Pardoll DM, Pan F and Topalian SL: Mechanisms regulating PD-L1 expression on tumor and immune cells. J Immunother Cancer 7: 305, 2019.
19. Iacovelli R, Nolè F, Verri E, Renne G, Paglino C, Santoni M, Cossu Rocca M, Giglione P, Aurilio G, Cullurà D, *et al*: Prognostic role of PD-L1 expression in renal cell carcinoma. A systematic review and meta-analysis. Target Oncol 11: 143-148, 2016.
20. Thompson RH, Dong H and Kwon ED: Implications of B7-H1 expression in clear cell carcinoma of the kidney for prognostication and therapy. Clin Cancer Res 13: 709s-715s, 2007.
21. Cheng SW, Chen PC, Lin MH, Ger TR, Chiu HW and Lin YF: GBP5 repression suppresses the metastatic potential and PD-L1 expression in triple-negative breast cancer. Biomedicines 9: 371, 2021.
22. Ghandi M, Huang FW, Jané-Valbuena J, Kryukov GV, Lo CC, McDonald ER III, Barretina J, Gelfand ET, Bielski CM, Li H, *et al*: Next-generation characterization of the cancer cell line encyclopedia. Nature 569: 503-508, 2019.
23. Tang Z, Kang B, Li C, Chen T and Zhang Z: GEPIA2: An enhanced web server for large-scale expression profiling and interactive analysis. Nucleic Acids Res 47 (W1): W556-W560, 2019.
24. Gumz ML, Zou H, Kreinest PA, Childs AC, Belmonte LS, LeGrand SN, Wu KJ, Luxon BA, Sinha M, Parker AS, *et al*: Secreted frizzled-related protein 1 loss contributes to tumor phenotype of clear cell renal cell carcinoma. Clin Cancer Res 13: 4740-4749, 2007.
25. von Roemeling CA, Radisky DC, Marlow LA, Cooper SJ, Grebe SK, Anastasiadis PZ, Tun HW and Copland JA: Neuronal pentraxin 2 supports clear cell renal cell carcinoma by activating the AMPA-selective glutamate receptor-4. Cancer Res 74: 4796-4810, 2014.
26. Lánczky A and Győrffy B: Web-based survival analysis tool tailored for medical research (KMplot): Development and implementation. J Med Internet Res 23: e27633, 2021.
27. Chandrashekar DS, Bashel B, Balasubramanya SAH, Creighton CJ, Ponce-Rodriguez I, Chakravarthi BVSK and Varambally S: UALCAN: A portal for facilitating tumor subgroup gene expression and survival analyses. Neoplasia 19: 649-658, 2017.
28. Vasaikar SV, Straub P, Wang J and Zhang B: LinkedOmics: Analyzing multi-omics data within and across 32 cancer types. Nucleic Acids Res 46 (D1): D956-D963, 2018.
29. Zhou Y, Zhou B, Pache L, Chang M, Khodabakhshi AH, Tanaseichuk O, Benner C and Chanda SK: Metascape provides a biologist-oriented resource for the analysis of systems-level datasets. Nat Commun 10: 1523, 2019.
30. Warde-Farley D, Donaldson SL, Comes O, Zuberi K, Badrawi R, Chao P, Franz M, Grouios C, Kazi F, Lopes CT, *et al*: The GeneMANIA prediction server: Biological network integration for gene prioritization and predicting gene function. Nucleic Acids Res 38 (Web Server Issue): W214-W220, 2010.
31. Li T, Fan J, Wang B, Traugh N, Chen Q, Liu JS, Li B and Liu XS: TIMER: A web server for comprehensive analysis of tumor-infiltrating immune cells. Cancer Res 77: e108-e110, 2017.
32. Li T, Fu J, Zeng Z, Cohen D, Li J, Chen Q, Li B and Liu XS: TIMER2.0 for analysis of tumor-infiltrating immune cells. Nucleic Acids Res 48 (W1): W509-W514, 2020.
33. Brodaczewska KK, Szczylik C, Fiedorowicz M, Porta C and Czarnecka AM: Choosing the right cell line for renal cell cancer research. Mol Cancer 15: 83, 2016.
34. Furge KA, Chen J, Koeman J, Swiatek P, Dykema K, Lucin K, Kahnoski R, Yang XJ and The BT: Detection of DNA copy number changes and oncogenic signaling abnormalities from gene expression data reveals MYC activation in high-grade papillary renal cell carcinoma. Cancer Res 67: 3171-3176, 2007.
35. Livak KJ and Schmittgen TD: Analysis of relative gene expression data using real-time quantitative PCR and the 2 (-Delta Delta C(T)) method. Methods 25: 402-408, 2001.
36. Cerezo M, Guemiri R, Druillennec S, Girault I, Malka-Mahieu H, Shen S, Allard D, Martineau S, Welsch C, Agoussi S, *et al*: Translational control of tumor immune escape via the eIF4F-STAT1-PD-L1 axis in melanoma. Nat Med 24: 1877-1886, 2018.
37. Cha JH, Chan LC, Li CW, Hsu JL and Hung MC: Mechanisms controlling PD-L1 expression in cancer. Mol Cell 76: 359-370, 2019.
38. Cerbone L, Cattrini C, Vallome G, Latocca MM, Boccardo F and Zanardi E: Combination therapy in metastatic renal cell carcinoma: Back to the future? Semin Oncol 47: 361-366, 2020.
39. Braun DA, Bakouny Z, Hirsch L, Flippot R, Van Allen EM, Wu CJ and Choueiri TK: Beyond conventional immune-checkpoint inhibition-novel immunotherapies for renal cell carcinoma. Nat Rev Clin Oncol 18: 199-214, 2021.
40. Wu T and Dai Y: Tumor microenvironment and therapeutic response. Cancer Lett 387: 61-68, 2017.
41. Gajewski TF, Schreiber H and Fu YX: Innate and adaptive immune cells in the tumor microenvironment. Nat Immunol 14: 1014-1022, 2013.
42. Dai S, Zeng H, Liu Z, Jin K, Jiang W, Wang Z, Lin Z, Xiong Y, Wang J, Chang Y, *et al*: Intratumoral CXCL13+CD8+T cell infiltration determines poor clinical outcomes and immunoevasive contexture in patients with clear cell renal cell carcinoma. J Immunother Cancer 9: e001823, 2021.
43. Giraldo NA, Becht E, Pagès F, Skliris G, Verkarre V, Vano Y, Mejean A, Saint-Aubert N, Lacroix L, Natario I, *et al*: Orchestration and prognostic significance of immune checkpoints in the microenvironment of primary and metastatic renal cell cancer. Clin Cancer Res 21: 3031-3040, 2015.
44. Giraldo NA, Becht E, Vano Y, Petitprez F, Lacroix L, Validire P, Sanchez-Salas R, Ingels A, Oudard S, Moatti A, *et al*: Tumor-infiltrating and peripheral blood T-cell immunophenotypes predict early relapse in localized clear cell renal cell carcinoma. Clin Cancer Res 23: 4416-4428, 2017.
45. Braun DA, Street K, Burke KP, Cookmeyer DL, Denize T, Pedersen CB, Gohil SH, Schindler N, Pomerance L, Hirsch L, *et al*: Progressive immune dysfunction with advancing disease stage in renal cell carcinoma. Cancer Cell 39: 632-648. e8, 2021.
46. Verhoeven Y, Tilborghs S, Jacobs J, De Waele J, Quatannens D, Deben C, Prenen H, Pauwels P, Trinh XB, Wouters A, *et al*: The potential and controversy of targeting STAT family members in cancer. Semin Cancer Biol 60: 41-56, 2020.
47. Zhu H, Wang Z, Xu Q, Zhang Y, Zhai Y, Bai J, Liu M, Hui Z and Xu N: Inhibition of STAT1 sensitizes renal cell carcinoma cells to radiotherapy and chemotherapy. Cancer Biol Ther 13: 401-407, 2012.
48. Kornepati AVR, Vadlamudi RK and Curiel TJ: Publisher correction: Programmed death ligand 1 signals in cancer cells. Nat Rev Cancer 22: 190, 2022.
49. Yi M, Niu M, Xu L, Luo S and Wu K: Regulation of PD-L1 expression in the tumor microenvironment. J Hematol Oncol 14: 10, 2021.
50. Zhang H, Zhu C, He Z, Chen S, Li L and Sun C: LncRNA PSMB8-AS1 contributes to pancreatic cancer progression via modulating miR-382-3p/STAT1/PD-L1 axis. J Exp Clin Cancer Res 39: 179, 2020.
51. Miao Q, Ge M and Huang L: Up-regulation of GBP2 is associated with neuronal apoptosis in rat brain cortex following traumatic brain injury. Neurochem Res 42: 1515-1523, 2017.